International Journal of Fracture **103:** 95–109, 2000.

Dynamic response of bimaterial and graded interface cracks under impact loading

PRABHAKAR R. MARUR and HAREESH V. TIPPUR*
Department of Mechanical Engineering, Auburn University, Auburn, Al 36849. e-mail: htippur@eng.auburn.edu

Received 22 March 1999; accepted in revised form 16 September 1999

Abstract. The interfacial fracture in bimaterial and functionally graded material (FGM) under impact loading conditions is investigated using experimental and numerical techniques that are valid for both type of interfaces. Experiments are conducted on epoxy based specimens in three point bend configuration and the complex SIF is measured using an electrical strain gage mounted close to the crack-tip. A complementary two-dimensional finite element simulation is performed using tup force and support reactions as input tractions, and the SIF-time history is determined using a displacement extrapolation technique. The experimentally determined SIF-histories match closely with numerical simulation up to the time of fracture initiation. The test results show that the mode-mixity remains nearly constant through out the test in both the materials, and the mixity values correspond to their respective static counterparts. The general dynamic response of the bimaterial and FGM specimens in terms of impact load, support reaction and the magnitude of complex SIF are comparable, and the mode-mixity is the parameter that distinguishes the graded interface from the bimaterial case.

Key words: Interface crack, complex stress intensity factor, bimaterial, functionally graded material (FGM), impact loading, strain gages, dynamic fracture.

1. Introduction

The fracture strength of the interface between dissimilar media plays an important role in the area of microelectronics, thin/thick film coatings, claddings, etc. The cladded and coated components that are subjected to high thermal gradients, the components become susceptible to cracking and spalling due to locked-in residual and thermal stresses owing to the thermal mismatch across the sharp interface. In the recent years, a new concept in joining dissimilar media has emerged to replace the sharp interface by an interlayer. The composition of the interlayer varies from one material to the other in a continuous manner. This new class of materials known as functionally graded material (FGM), have been introduced in higher temperature and wear applications: see (Yamanouchi et al., 1990; Erdogan, 1995) for review, applications and other related references on FGM.

Many investigators have conducted static fracture experiments on bimaterial systems and have measured fracture toughness for different material combinations and mode-mixities (Charalambides et al., 1989; Cao and Evans, 1989). Dynamic fracture experiments on bimaterials are limited due to the complexity of testing and analysis of the results. Transient testing of bimaterial cracks has been reported by Tippur and Rosakis (1991); Liu et al. (1993) and Singh and Shukla (1997).

The experimental work on fracture of FGM is rather limited at the moment. The dependence of fracture toughness on the spatial position of the crack within the graded region

* Corresponding author: (e-mail address: htippur@eng.auburn.edu)

coupled with complex microstructure of FGM poses a challenge in the experimental investigation of FGM. Fukui et al. (1997) have conducted three-point bend testing of Al-Al_3Ni based FGM, and studied the variation of fracture strength with the volume fraction of Al_3Ni phase at the crack initiation plane. Sarkar et al. (1997) used micro-indentation to track the fracture toughness variation across the composition profiles of Al_2O_3 based FGM. The dynamic fracture experiments on FGM are scarce, and only reference cited in the literature surveyed is by Parameswaran and Shukla (1998), who have studied the dynamic fracture of layered FGM using photoelastic technique.

By considering the material gradient near the tip of an interface crack in the analytical modeling, the physically inadmissible oscillations in stresses and displacements predicted by linear elastic theory are removed. This model could be applied to bimaterial systems also, as bonding processes in general would lead to very steep, nevertheless continuous variation of material properties across the interface due to diffusion and interpenetration. Hence the study of crack in a graded interface would enhance the understanding of the fracture in a generic material, as the fracture behavior of FGM would be analogous to that of bimaterial or homogenous medium depending on the material gradient across the crack. In a recent paper (Marur and Tippur, 1999b), the authors have presented numerical analyses of the singular field around a crack in FGM under static loading, and compared the fracture parameters with that of the homogeneous and bimaterial cracks. Their analysis has shown that the fracture parameters of FGM approach that of the bimaterial as the material gradient is increased. And for a given material gradient near the crack-tip, the magnitude of SIF of FGM is comparable to that of the bimaterial crack, while significant differences are seen in the mode-mixity. The mode-mixity (ratio of sliding and opening fracture modes) plays an important role in the characterization of bimaterial system, and strongly influences the fracture toughness of the interface. Hence, it would be of importance to investigate the fracture behavior of FGM and bimaterial under dynamic loading conditions and study the variation of mode-mixity in both material types.

The intent of this paper is to study the influence of material gradient on the impact response of the crack in bimaterial and FGM. Low-velocity impact experiments conducted on bimaterial and FGM specimens fabricated from epoxy and glass-filled epoxy materials. The specimens are tested in three-point bend configuration in a specially designed drop-tower system. The test results are complimented by two-dimensional finite element simulations performed using the measured interaction forces as traction boundary conditions. The numerical and experimental results are obtained using techniques that are unified for both type of interfaces, permitting a direct comparison of the test results. A nodal displacement extrapolation technique is used to compute complex SIF in the numerical simulations, and electrical strain gages are used for experimental determination of the fracture parameters. The details of the impact tests and the numerical simulations are presented in the following sections.

2. Interface fracture mechanics

2.1. BIMATERIAL CRACK

Consider a crack on an interface between two homogeneous isotropic materials as shown in Figure 1(a). The asymptotic near-tip field can be expressed in terms of the complex stress intensity factor $\mathbf{K} = K_1 + iK_2$ as

$$\sigma_{ij} \sim \frac{1}{\sqrt{r}}[K_1 \Sigma_{ij}^{\mathrm{I}}(\theta, \ln r; \varepsilon) + K_2 \Sigma_{ij}^{\mathrm{II}}(\theta, \ln r; \varepsilon)], \quad i, j = x, y, \tag{1}$$

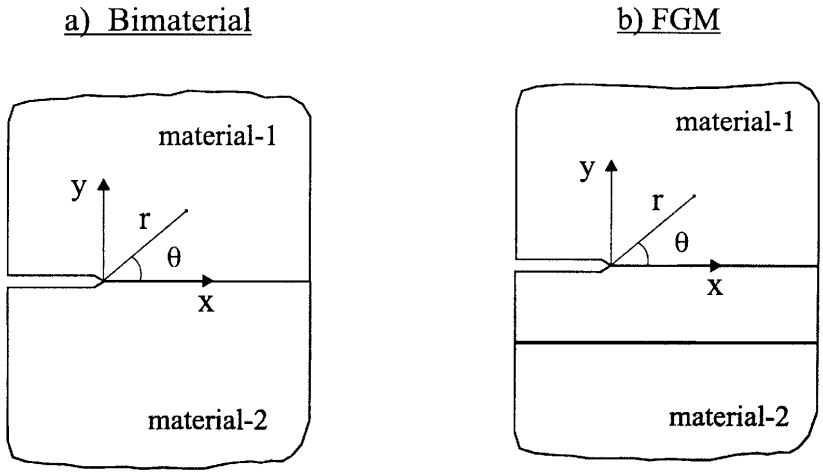

Figure 1. Interface crack in bimaterial and FGM.

where, ε is the bimaterial constant and Σ_{ij}^{I} and $\Sigma_{ij}^{\mathrm{II}}$ are the angular functions associated with the K-dominant terms. By setting the material mismatch to zero, the complex SIF reduces to $K_{\mathrm{I}} + iK_{\mathrm{II}}$, where K_{I} and K_{II} are the SIFs associated with pure mode-I and mode-II loading and Σ_{ij}^{I} and $\Sigma_{ij}^{\mathrm{II}}$ degenerate to the standard angular functions for the homogeneous medium. The ratio of the individual SIF components is denoted as mode-mixity and it can be given using the arbitrary length parameter L introduced by Rice (1988) as

$$\psi_b = \tan^{-1}\left[\frac{\Im(\mathbf{K}L^{i\varepsilon})}{\Re(\mathbf{K}L^{i\varepsilon})}\right]. \tag{2}$$

Following Sun and Jih (1987), the value of L is set to $2a$, where a is the crack length.

2.2. Crack in FGM

Consider a crack lying in the interlayer between the two dissimilar media as shown in Figure 1(b). Jin and Noda (1993) have shown that the stress field around the crack tip in FGM is identical to that in homogeneous medium if the material properties are continuous and piecewise continuously differentiable. Therefore the singular stresses near the crack tip can be given as

$$\sigma_{ij} = \frac{1}{\sqrt{2\pi r}}[K_{\mathrm{I}} f_{ij}^{\mathrm{I}}(\theta) + K_{\mathrm{II}} f_{ij}^{\mathrm{II}}(\theta)], \quad i, j = x, y, \tag{3}$$

where $f_{ij}^{\mathrm{I}}(\theta)$ and $f_{ij}^{\mathrm{II}}(\theta)$ are standard angular functions for a crack in a homogeneous elastic medium.

In FGM, when the crack is not parallel to the material gradient, both normal and shear tractions occur ahead of the crack tip, regardless of the remote loading conditions due to the nonsymmetry in the material properties. Hence, the complex SIF introduced in the context of a bimaterial crack can be used to measure the field in FGM and it can be given as $\mathbf{K} = K_{\mathrm{I}} + \imath K_{\mathrm{II}}$ or alternatively as $\mathbf{K} = |K|\mathrm{e}^{\imath\psi}$, where

$$\psi = \tan^{-1}\frac{K_{\mathrm{II}}}{K_{\mathrm{I}}}. \tag{4}$$

Due to the regular singularity at the crack tip in FGM, the phase angle definition does not require an arbitrary length parameter.

3. Computational model

The magnitude of SIF and the mode-mixity are computed by extrapolating the nodal displacements extracted from the finite element analysis. The asymptotic displacement equations derived for bimaterial crack are used in the extrapolation technique and the formulation can be applied to homogeneous and FGM cases by letting $\varepsilon = 0$ in the computation. Only the outline of the procedure is described and the details can be found in (Marur and Tippur, 1999a).

The magnitude of complex stress intensity factor is related to complex crack opening displacement $\boldsymbol{\delta}(= \Delta v + \imath \Delta u)$ through

$$|\boldsymbol{\delta}| = \gamma |\mathbf{K}| \sqrt{2\pi r}, \tag{5}$$

where γ reflects the material properties of the bulk materials. From regression analysis of the above equation, the absolute value of $\mathbf{K}$ can be obtained.

The mode-mixity can be computed from the ratio of SIFs as

$$\frac{K_2}{K_1} = \frac{[F_2(\phi)/F_1(\phi)](\Delta u/\Delta v) - 1}{(\Delta u/\Delta v) + [F_2(\phi)/F_1(\phi)]}, \tag{6}$$

where

$$F_1(\phi) = \sin(\phi) - 2\varepsilon \cos(\phi),$$

$$F_2(\phi) = \cos(\phi) + 2\varepsilon \sin(\phi),$$

$$\phi = \varepsilon \log(r/2a).$$

Considering only the displacements of nodes that are outside the oscillatory region, an extrapolation technique can be used to fit a linear equation to the K_2/K_1 values to compute mode-mixity in the limit $r \to 0$. The extrapolation technique has been calibrated for different material combinations under static loading conditions (Marur and Tippur, 1999a).

To demonstrate the accuracy of this extrapolation scheme in the dynamic loading conditions, a bench mark problem which has an analytical solution (Thau and Liu, 1971) is solved. The problem considered is a slanted crack in a constrained homogeneous plate subjected to step load at the boundary as shown in Figure 2. The finite element mesh is created with 8-noded quadrilateral elements, and an uniformly distributed load is applied at the boundary. Explicit time-integration scheme is used in the solution and at each time step the SIF components are computed. The time variation of dynamic K_{I} and K_{II} are shown in Figure 3. The present results are in good agreement with the analytical solution until the reflected stress waves arrive at the crack tip at 10 μs.

4. Strain gage technique

The strain gage method described here can be used for homogeneous and FGM cases by setting the bimaterial constant ε to zero. Only a brief description of the technique is presented here, and the details can be found in (Marur and Tippur, 1999a).

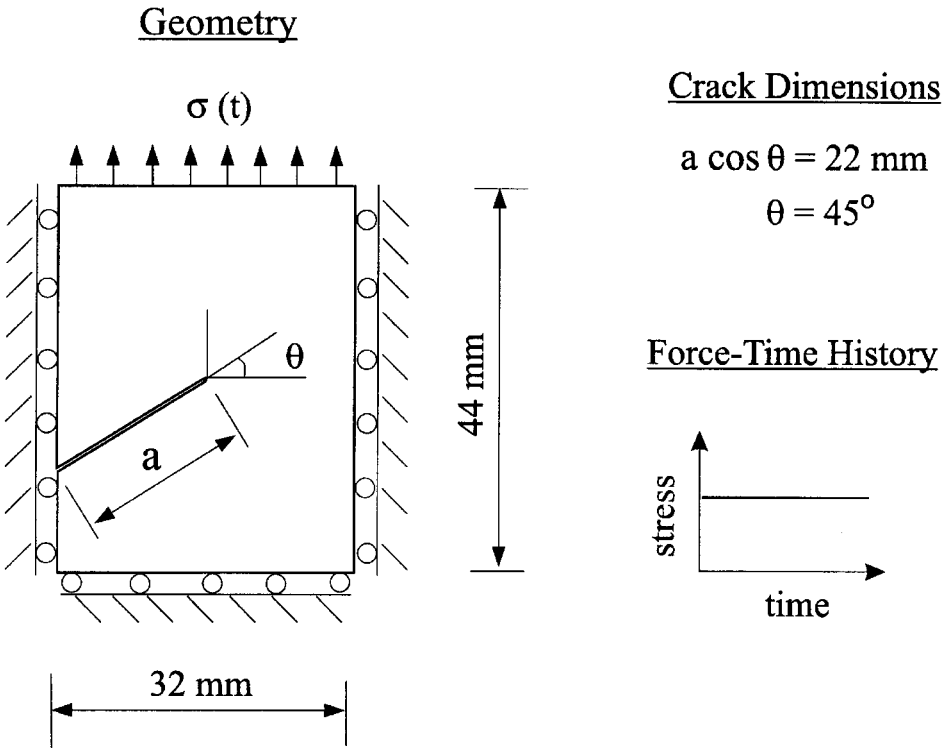

Figure 2. Specimen geometry and load-time history. All dimensions are in mm.

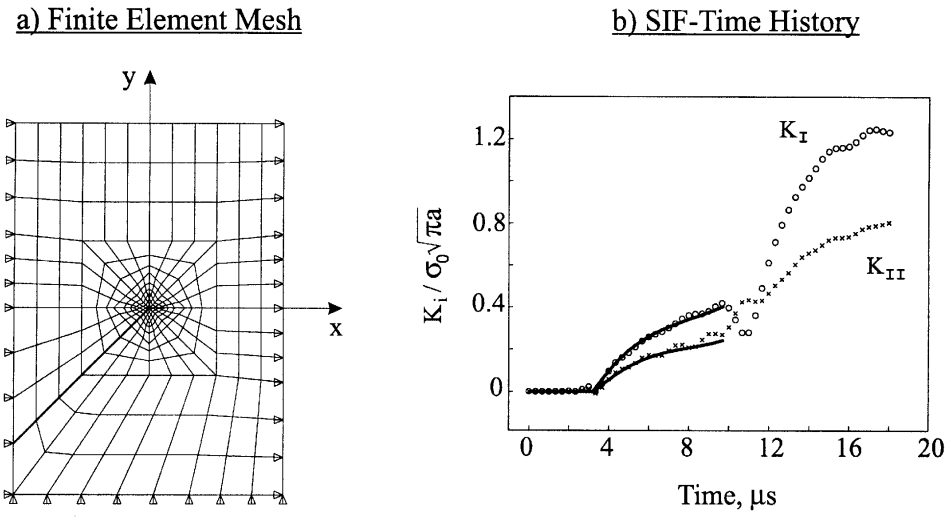

Figure 3. The finite element discretization and the SIF-time histories. –: Thau and Liu, 1971; ○: present FEA.

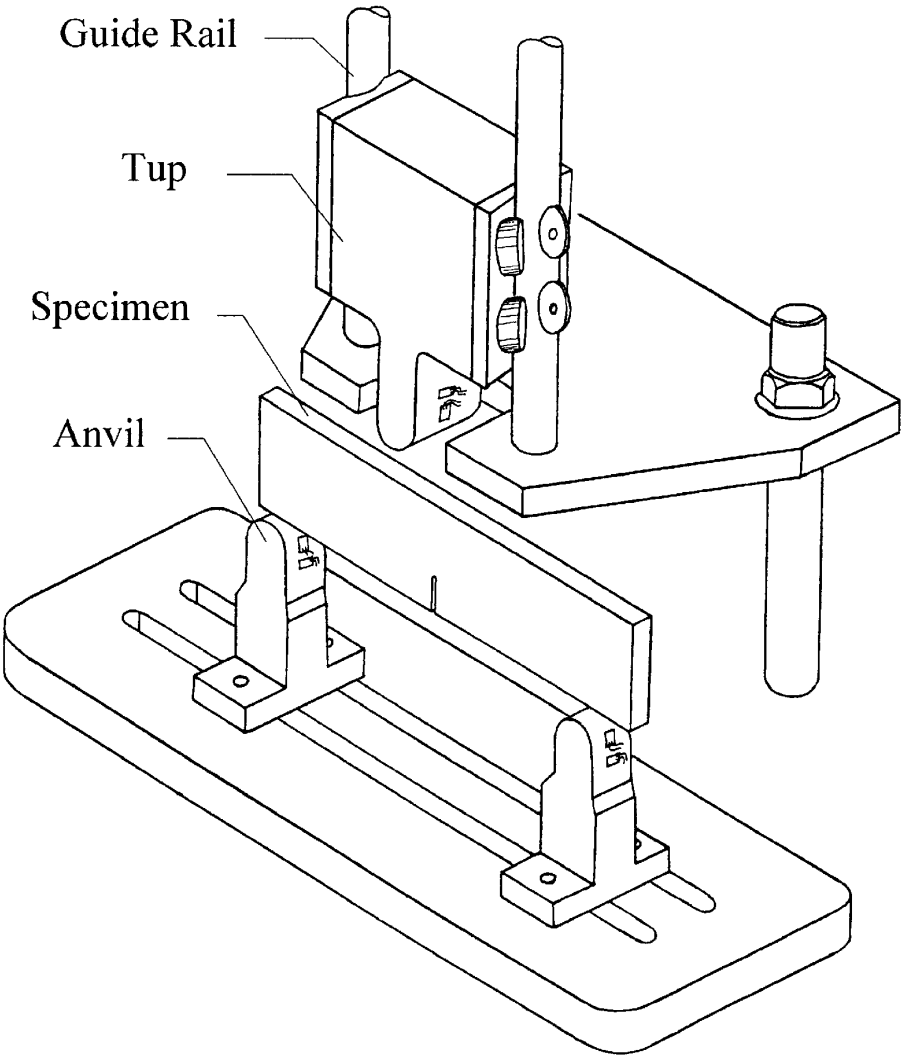

Figure 4. Schematic of the drop-tower loading system.

The radial and hoop strain around the crack tip under plane stress conditions can be given using big-O notation as

$$E\varepsilon_{rr} = r^{-1/2}[K_1(\Sigma^{\mathrm{I}}_{rr} - \nu\Sigma^{\mathrm{I}}_{\theta\theta}) + K_2(\Sigma^{\mathrm{II}}_{rr} - \nu\Sigma^{\mathrm{II}}_{\theta\theta})] + O(r), \tag{7}$$

$$E\varepsilon_{\theta\theta} = r^{-1/2}[K_1(\Sigma^{\mathrm{I}}_{\theta\theta} - \nu\Sigma^{\mathrm{I}}_{rr}) + K_2(\Sigma^{\mathrm{II}}_{\theta\theta} - \nu\Sigma^{\mathrm{II}}_{rr})] + O(r). \tag{8}$$

In the above equations, only the compliant half-plane of the bimaterial system is considered and hence the Young's modulus and Poisson's ratio are given in a generic fashion without subscripts. The influence of higher order terms is taken as correction factor which is computed as the difference between the K-dominant solution and the higher-order solution. The correction factor is applied to the measured strain to obtain the corrected strain $\tilde{\varepsilon}_{ij}$ from which SIF can be computed as

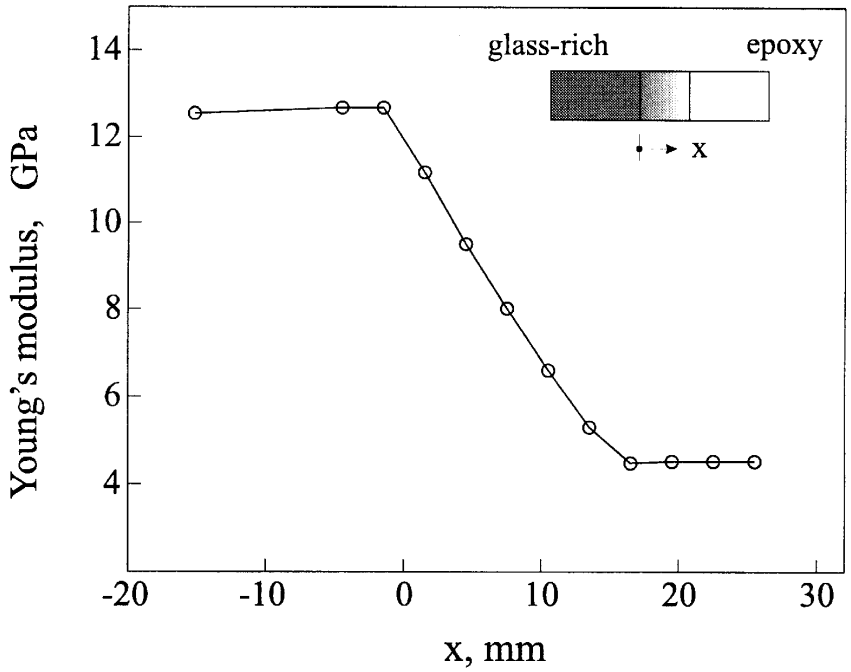

Figure 5. Variation of dynamic Young's modulus in FGM.

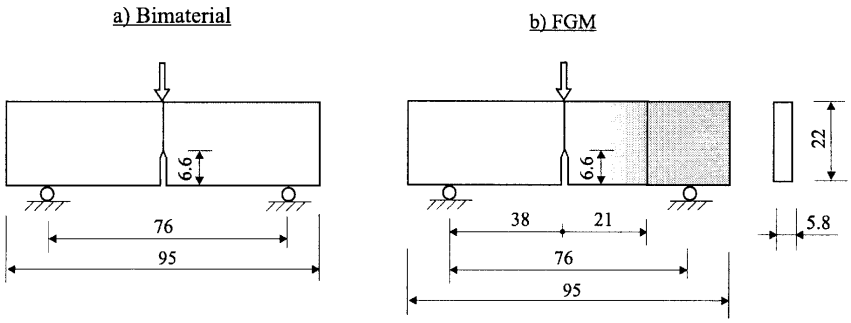

Figure 6. Specimen geometry. All dimensions in mm.

$$\left\{ \begin{array}{c} K_1 \\ K_2 \end{array} \right\} = E\sqrt{r} \left[\begin{array}{cc} (\Sigma^{\mathrm{I}}_{rr} - \nu\Sigma^{\mathrm{I}}_{\theta\theta}) & (\Sigma^{\mathrm{II}}_{rr} - \nu\Sigma^{\mathrm{II}}_{\theta\theta}) \\ (\Sigma^{\mathrm{I}}_{\theta\theta} - \nu\Sigma^{\mathrm{I}}_{rr}) & (\Sigma^{\mathrm{II}}_{\theta\theta} - \nu\Sigma^{\mathrm{II}}_{rr}) \end{array} \right]^{-1} \left\{ \begin{array}{c} \tilde{\varepsilon}_{rr} \\ \tilde{\varepsilon}_{\theta\theta} \end{array} \right\}. \tag{9}$$

The radial and hoop strains are measured by mounting a biaxial strain rosette near the crack tip. The strain gage must be located in the region prescribed by $r \geqslant 0.5B$, where B is the thickness of the specimen and $30^\circ \geqslant \theta \leqslant 150^\circ$ for plane stress conditions to prevail (Sinha et al., 1997). Within this zone, r and θ must be chosen such that the coefficient matrix in the above equation is well conditioned and the sensitivity of measurement is maximized. For most common values of ε and ν, the angles from 85° to 100° provide best conditioning of the matrix and peak strains occur in the neighborhood of $\theta = 90^\circ$. Hence, the strain rosette is mounted at $r = 0.6B$ and $\theta = 90^\circ$ on the compliant side of the specimen.

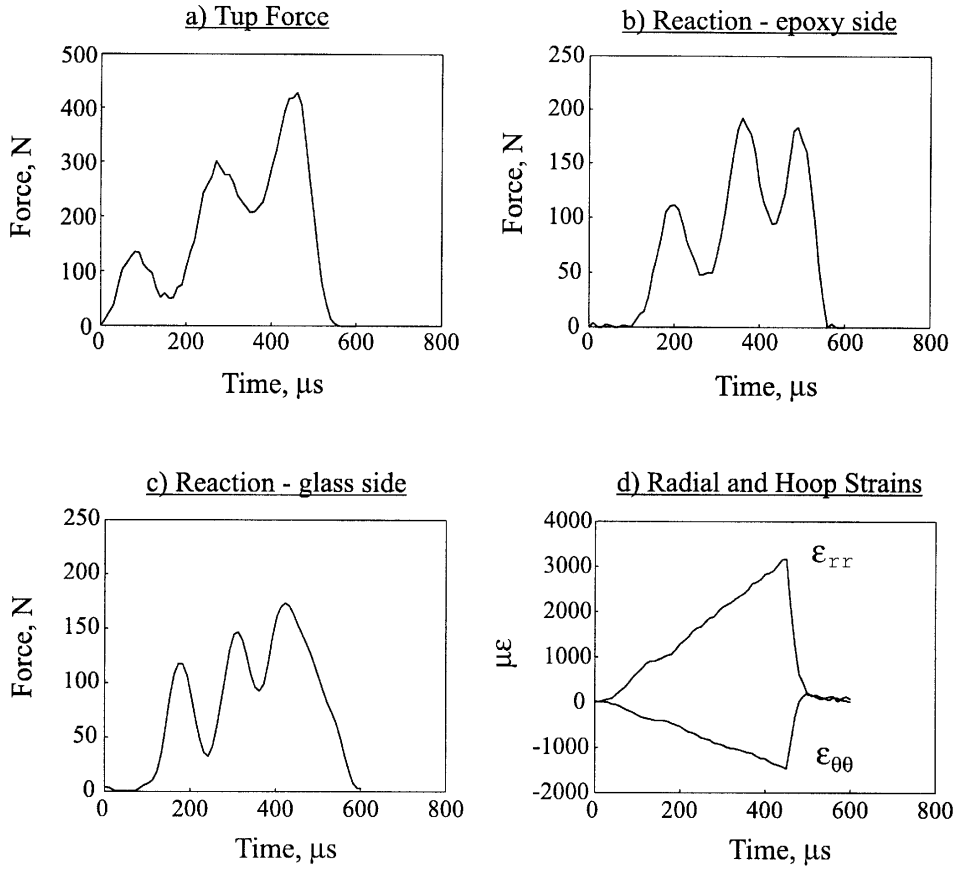

Figure 7. Measured data for impact testing of bimaterial specimens.

5. Experimental procedure

5.1. Drop-tower system

The bimaterial and FGM specimens are tested in a drop-tower system in three point bending configuration. The schematic of the test setup is shown in Figure 4. The guide rails are made of hardened and polished stainless steel, and the tup glides down the rails on four angled roller-bearings ensuring tup alignment and reducing frictional losses. The mass of the impactor is concentrated at the center, eliminating the vibration of the impactor. The anvils are adjustable, thus accommodating specimens of different spans. The tup and the anvils are instrumented with electrical strain gages.

The signals from the gages are amplified by high-frequency amplifiers having a frequency response of 200 kHz-3dB at 1000X amplification. The amplified signals are then acquired by a 8-channel, 1-MHz data acquisition card. The tup activates an optical switch at the time of impact to trigger data acquisition.

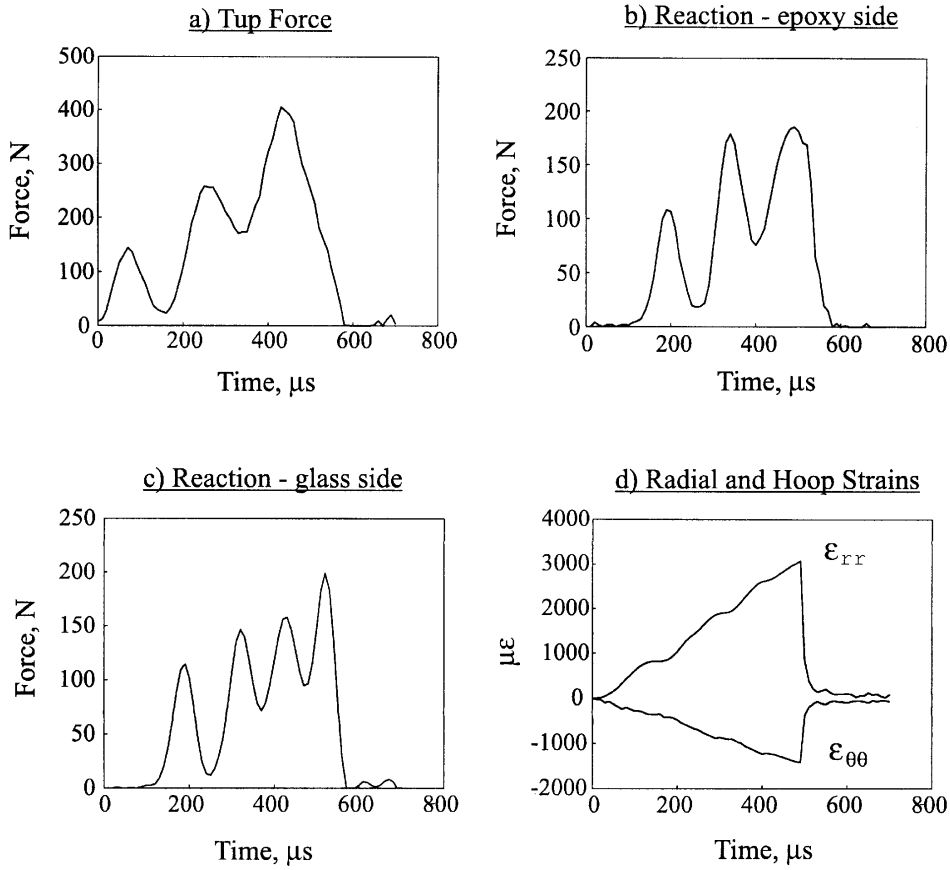

Figure 8. Impact test data for a FGM specimen.

5.2. SPECIMEN FABRICATION

The interface specimens tested in this study are fabricated from a two-part slow curing epoxy, with and without fillers. Uncoated solid glass spheres with mean diameter of 33μm are used as fillers. The volume fraction of the glass spheres reaches 53 percent in the glass-filled epoxy samples. All the test specimens are cast from a single batch of epoxy resin to reduce the variation in the material properties among the specimens. The physical properties of the bulk materials are listed in Table 1.

The bimaterial specimens are fabricated by joining pure epoxy and glass-filled epoxy specimen halves with epoxy resin. The bonding surfaces are roughened with 240-grit emery paper, and the surfaces are subsequently cleaned with isopropyl alcohol. The specimen halves are then positioned in an acrylic mould and kept in place under light clamping pressure. The samples are allowed to cure for at least seven days.

The FGM specimens are fabricated by a three step process. First, the gradient interlayer of about 15 mm to 21 mm in width, with properties varying from pure-epoxy to glass-rich epoxy, is obtained using the gravity-assisted casting technique (Marur and Tippur, 1998). Then the interlayer is placed in an acrylic mould in such a way that the epoxy surface is exposed. Then unfilled-epoxy is poured into the mould and allowed to cure for two days. The sample is then removed and kept reversed in the mould to expose the glass-rich side. Then epoxy mixed with

Table 1. Dynamic material properties

Specimen	E, GPa	$-\nu$	ρ, kg/m^3
Epoxy	4.6	0.37	1150
Glass-filled epoxy	13.0	0.32	1720

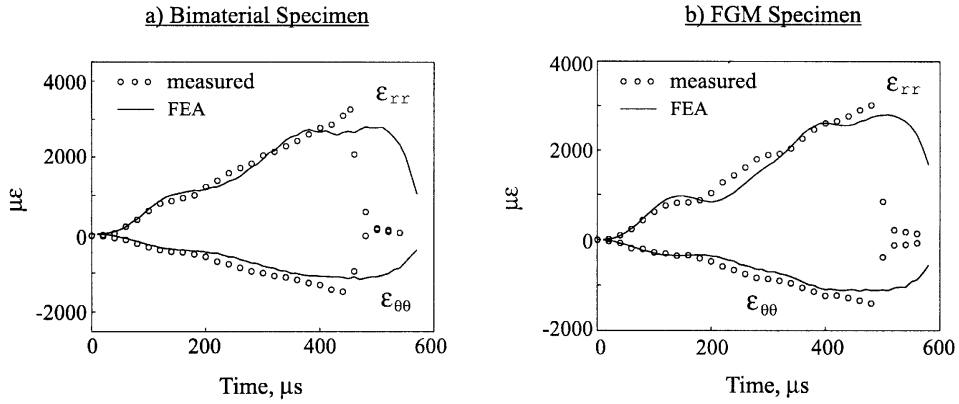

Figure 9. Comparison of measured strains with finite element simulation.

glass spheres (reaching a volume fraction of 53 percent) is poured, and allowed to cure for a week.

The variation of dynamic elastic properties in the gradient region is determined using a recently developed measurement technique involving ultrasonic wave velocity and local contact stiffness measurements (Marur and Tippur, 1998). The Poisson's ratio variation is linear in the graded zone, with the upper and lower limits at 0.35 and 0.28 for epoxy and glass-filled epoxy, respectively. The dynamic Young's modulus variation in the gradient region is shown in Figure 5. It can be observed from the figure that the variation of modulus within the gradient region is quite linear.

The samples are machined to the final dimensions as shown in Figure 6. A notch of $0.3W$ length, where W is the width of the specimen, is machined in a milling machine with a special 0.15 mm-thick slitter. In the case of FGM, the notch is machined at the interface between the epoxy and the gradient region.

5.3. Dynamic fracture tests

The specimens are tested in the drop tower with the initial impact velocity of 0.5 m/s. A biaxial rectangular rosette (CEA-13-032WT-120, Measurements Group Inc.) is mounted at 3.5 mm ($= 0.6B$) and $\theta = 90°$. The interaction forces, and the strain signals from the test specimen are recorded in each test. The measured time histories for the bimaterial sample are shown in Figure 7. The results obtained for the FGM specimen are shown in Figure 8.

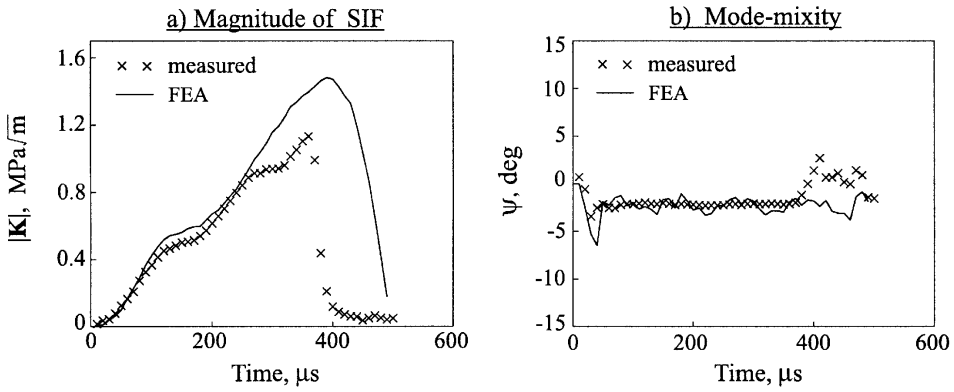

Figure 10. Comparison measured fracture parameters with numerical simulation for the bimaterial specimen.

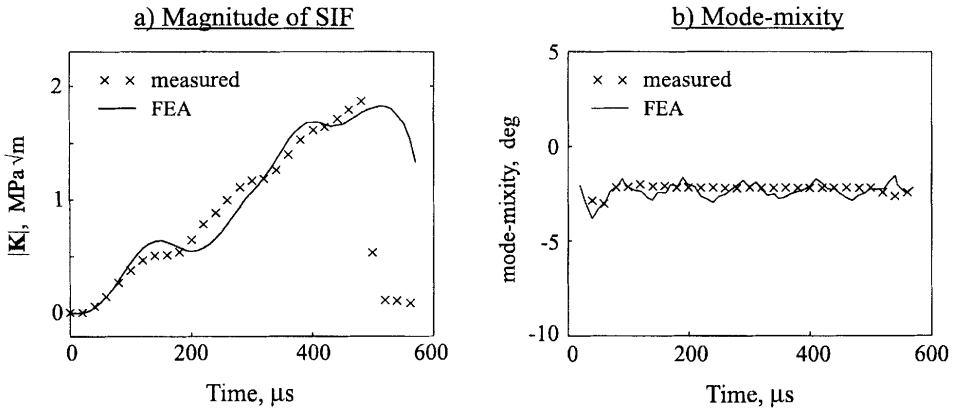

Figure 11. Comparison measured fracture parameters with numerical simulation for the FGM specimen.

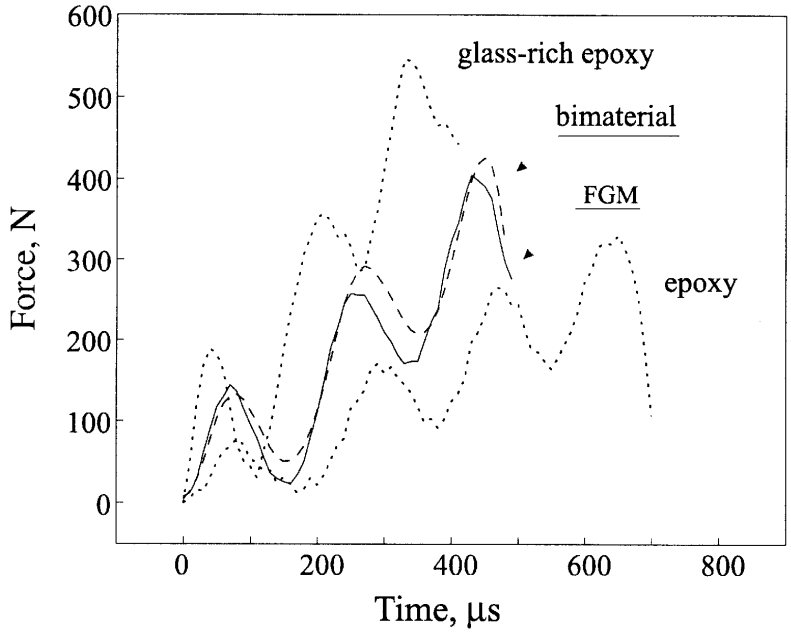

Figure 12. Comparison of time-variation of tup forces.

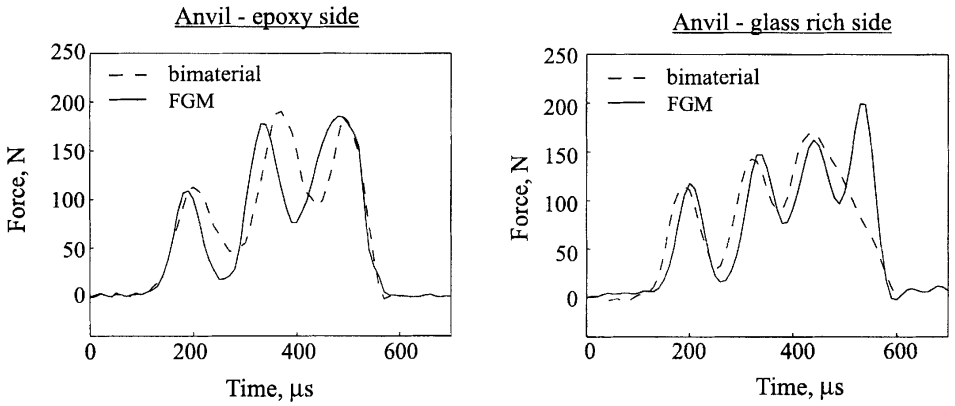

Figure 13. Comparison of time-variation of support reaction of bimaterial and FGM.

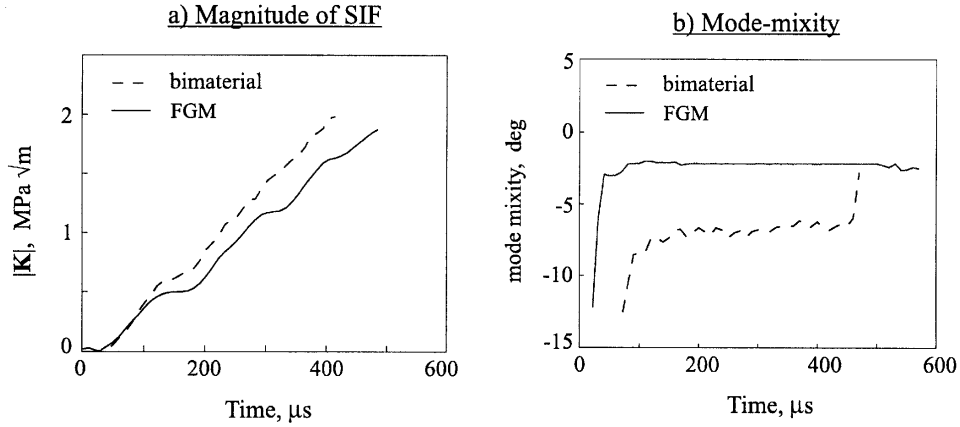

Figure 14. Comparison of fracture parameters of bimaterial and FGM.

6. Numerical simulation

The dynamic fracture tests are simulated using a 2-dimensional finite element model. A rectangular mesh with 8-noded isoparameteric elements with 2-degrees of freedom at each node is used in the analysis. The finite element mesh is created in such a way that the elements in the gradient region are grouped into narrow parallel strips perpendicular to the direction of material variation to facilitate material property modification. The material gradient is achieved by selectively changing the material properties of the elements in the graded region in accordance with the form of property variation desired using a pre-processor code. In this work, linear material property variation in the graded zone is used as it closely matches the property variation in the FGM specimens.

The measured tup force and support reaction time histories are applied as traction boundary conditions to the finite element model. The full length of the specimen (including the overhangs) is modeled without imposing any displacement constraints. Explicit time-integration scheme is used in the analysis and at each time step, radial and hoop strains from a node placed at 3.5 mm from the crack-tip (corresponding to the strain gage location) are extracted.

The computed strains are compared with the measured data in Figure 9 for both FGM and bimaterial specimens. The agreement between the measured and computed strains is good

until the time of fracture. The measured strain-time histories are transformed to complex SIF-time histories using (9). The magnitude of the complex SIF and the mode-mixity are compared with the numerical simulation in Figure 10 for the bimaterial specimen. The simulated data match well with the measured SIF until the time of fracture initiation. The mode-mixity remains between -6.3° and -6.7° throughout the test, which is quite close to the static value of -6.6°, which is computed by running a static loading case with the same mesh. In the initial stages, the mode-mixity shows instability because it is computed by taking the ratio of small values. Similar comparison between measured data and computed results for FGM is shown in Figure 11. The experimental values are in good agreement with the simulation until the time of fracture initiation. From Figure 11(b), it can be observed that the mode-mixity remains nearly constant at -3°, which is comparable to the static value of -2.75°.

7. Comparison of time-histories

The tup force, anvil reaction and SIF data of bimaterial and FGM are compared in this section. Since bimaterial and FGM specimens are obtained by joining two homogeneous materials, and it is likely that their impact behavior would be an intermediatory between the general dynamic behavior of the homogeneous materials.

Figure 12 shows the comparison of tup forces recorded for bimaterial and FGM. The tup force histories recorded for homogeneous epoxy and glass-filled epoxy specimens are also plotted in the figure for reference. The oscillations seen in the tup force are due to the contact stiffness at the impact point. As the contact stiffness increases, the overall slope of the force-time curve and the frequency of oscillations increase. The tup forces for bimaterial and FGM specimens are between that measured for epoxy and glass-rich specimens as expected. The anvil reactions recorded for FGM and bimaterial are compared in Figure 13. From Figures 12 and 13, it can be observed that the interaction force histories of the bimaterial and FGM are comparable.

The magnitude and phase of the complex SIF of bimaterial and FGM are compared in Figure 14. It can be seen from Figure 14(a) that the general variation of the magnitude of SIF in bimaterial and FGM are quite similar. In Figure 14(b), the mode mixity remains nearly constant through out the impact duration in both bimaterial and FGM samples, however the amplitudes are distinctly different. The mode-mixity of bimaterial is more than twice of that in FGM, and this difference is maintained until the time fracture initiation. It is instructive to note that the comparison of mode-mixities in Figure 14(b) is not unique owing to the use of arbitrary length parameter in the definition of mode-mixity for the bimaterial crack. However, the comparison is attempted in this paper as the length parameter has very weak influence on the computed SIF values and hence on mode-mixity, which is in line with the analytical results published by Rice (1988).

Under static loading conditions, it has been shown that the mode-mixity is strongly influenced by the material gradient in FGM, and for a given material gradient in FGM, the mode-mixity is the fracture parameter that distinguished the nature of the interface (Marur and Tippur, 1999b). The results of the present investigation show that the same argument holds true even with dynamic loading. The differences seen in the impact and support reaction are within the spread that would normally occur in the dynamic testing of identical specimens of same material. Hence the dynamic response of the crack in the FGM in tensile dominated

loading does not differ significantly from the bimaterial system, except for the reduction in the mode-mixity.

8. Conclusions

The dynamic response of interface cracks under low-velocity impact loading is investigated using experimental and numerical techniques. Impact experiments are conducted on epoxy based bimaterial and FGM specimens in three point bend configuration using drop-weight loading. Electrical strain gages mounted close to the crack-tip are used to determine the complex SIF. The measured impact force and the anvil reactions are applied as input tractions to a finite element model, and the fracture parameters are computed at each time step by extrapolation of crack flank displacements. The experimentally determined strain and SIF-histories match closely with numerical simulation upto the time-of-fracture initiation in both material types. The mode-mixity remains nearly constant through out the test in both the materials, and the mixity values are close to the respective static values. Between FGM and bimaterial, there are no significant differences in the dynamic response except for the reduction in the mode-mixity in FGM.

Acknowledgements

The support of this research by NSF Mechanics & Materials Program (CMS-9622055) is gratefully acknowledged.

References

Cao, H.C. and Evans, A.G. (1989). Experimental study of the fracture resistance of bimaterial interfaces. *Mechanics of Materials* **7**, 295–304.

Charalambides, P.G., Lund, J., Evans, A.G. and McMeeking, R.M. (1989). A test specimen for determining the fracture resistance of bimaterial interfaces. *Journal of Applied Mechanics* **56**, 77–82.

Erdogan, F., (1995). Fracture mechanics of functionally graded materials. *Composites Engineering*, **5**, 753–770.

Fukui, Y., Yamanaka, N. and Enokida, Y. (1997). Bending strength of an Al-Al_3Ni functionally graded material Composites B: *Engineering* **28**, 37–43.

Jin, Z.-H. and Noda, N. (1993). An internal crack parallel to the boundary of a non-homogeneous half plane under thermal loading. *International Journal Engineering Science* **31** 793–806.

Liu, C., Lambros, J. and Rosakis, A.J. (1993). Highly transient elastodynamics crack growth in a bimaterial interface: Higher order asymptotic analysis and optical measurements. *Journal of the Mechanics and Physics of Solids* **41**, 1857–954.

Marur, P.R. and Tippur, H.V. (1999a). A strain gage method for determination of fracture parameters in bimaterial systems. *Engineering Fracture Mechanics*, Vol. 64, No. 1, pp. 87–104.

Marur, P.R. and Tippur, H.V. (1999b). Numerical analysis of crack-tip fields in functionally graded materials with a crack normal to the elastic gradient. *International Journal of Solids and Structures* (to appear).

Marur, P.R. and Tippur, H.V. (1998). Evaluation of mechanical properties of functionally graded materials. *Journal of Testing and Evaluation* **26**, 539–545.

O'Dowd, N.P., Shih, C.F. and Stout, M.G. (1992). Test geometries for measuring interfacial fracture toughness. *International Journal of Solids and Structures* **29**, 571–589.

Parameswaran, V. and Shukla, A. (1998). Dynamic fracture of a functionally gradient material having discrete property variation, *Journal of Materials Science* **33**, 3303–3311.

Rice, J.R. (1998). Elastic fracture mechanics concepts for interface crack, *Journal of Applied Mechanics* **55**, 98–103.

Sarkar, P., Datta, S. and Nicholson, P.S. (1997). Functionally graded ceramic/ceramic and metal/ceramic composites by electrophoretic deposition. *Composites B: Engineering*, **28**, 49–56.

Singh, R.P. and Shukla, A. (1997). Subsonic and transonic crack growth along a bimaterial interfaces. *International Journal of Solids and Structures* **83**, 291–304.

Sinha, J.K., Tippur, H.V. and Xu, L. (1997). An interferometric and finite element investigation of interfacial crack-tip fields: Role of mode-mixity on 3-dimensional stress variations. *International Journal of Solids and Structures* **34**, 741–754.

Sun, C.T. and Jih, C.J. (1987). On strain energy release rates for interfacial cracks in bi-material media. *Engineering Fracture Mechanics* **28**, 13–20.

Thau, S.A. and Liu, T.H. (1971). Transient stress intensity factors for a finite crack in an elastic solid caused by a dilatational wave. *International Journal of Solids and Structures* **7**, 731–750.

Tippur, H.V. and Rosakis, A.J. (1991). Quasi-static and dynamic crack growth along bimaterial interfaces: A note on crack tip measurements using coherent gradient sensing. *Experimental Mechanics* **33**, 243–252.

Yamanouchi, M., Koizumi, M., Hirai, T. and Shiota, I. (1990). *FGM-90. Proc. First International Symposium on Functionally Graded Materials*, FGM Forum, Tokyo, Japan.